# Micro-impedance cytometry for detection and analysis of micron-sized particles and bacteria

**Catia Bernabini, David Holmes† and Hywel Morgan**

*Received 13th June 2010, Accepted 4th October 2010*
**DOI: 10.1039/c0lc00099j**

The sensitivity of a microfluidic impedance flow cytometer is governed by the dimensions of the sample analysis volume. A small volume gives a high sensitivity, but this can lead to practical problems including fabrication and clogging of the device. We describe a microfluidic impedance cytometer which uses an insulating fluid to hydrodynamically focus a sample stream of particles suspended in electrolyte, through a large sensing volume. The detection region consists of two pairs of electrodes fabricated within a channel 200 μm wide and 30 μm high. The focussing technique increases the sensitivity of the system without reducing the dimensions of the microfluidic channel. We demonstrate detection and discrimination of 1 μm and 2 μm diameter polystyrene beads and also *Escherichia coli*. Impedance data from single particles are correlated with fluorescence emission measured simultaneously. Data are also compared with conventional flow cytometry and dynamic light scattering: the coefficient of variation (CV) of size is found to be comparable between the systems.



## Introduction

Microfluidic devices have been developed that can analyse the dielectric properties of single particles in suspension at high speed.[1–10] Particles flow between pairs of micron-sized planar electrodes fabricated within a microfluidic channel. The electrodes are energised with an AC voltage and as particles pass between electrodes the change in the current flowing between the electrodes is measured and analysed to provide information on the size and dielectric properties of the particles.

Such devices have been able to discriminate different micron sized objects including beads (according to size[2,3,9]) and cells according to size and membrane properties.[5–7,9–10] A number of issues limit the sensitivity and specificity of these systems. Fundamentally the sensitivity is governed by the ratio of particle volume to the volume occupied by the electric field, defined as the volume fraction occupied by the particle, which should be maximised. In addition, the spatial location of each particle needs to be controlled accurately within the field. It is also important to ensure that only one particle at a time enters the detection region. Therefore, an efficient and accurate method for focussing particles into the centre of the electric field is important. One way to improve the sensitivity of the system is to reduce the dimensions of the channel. Typically for cell analysis, channels that are 30 μm to 40 μm in width and height are used. In order to measure smaller objects such as bacteria, the channel dimensions and electrode width should be reduced, for example to 5 μm, but this makes fabrication more difficult and greatly increases the likelihood of blockage of the channel.

*School of Electronics and Computer Science, University of Southampton, Highfield, Southampton, SO17 1BJ, UK. E-mail: hm@ecs.soton.ac.uk; Fax: +44 (0)2380 593029; Tel: +44 (0)2380 593330*
† Present address: London Centre for Nanotechnology, University College London, 17-19 Gordon Street Building, London, WC1H 0AH, UK.

Detection of sub-micron particles has been performed using nanopores, with sizes ranging from hundreds of nanometres to a few microns. These systems operate like a Coulter counter, where an electrical current passing through the channel is modulated by the presence of a particle in the channel. This resistive pulse technique was recently employed to detect 520 nm diameter particles flowing in a microfluidic channel with an aperture of $50 \times 16 \times 20\ \mu m^3$.[11] The method has been used to detect colloids,[12,13] viruses,[14] antibodies,[15] and single molecules.[16]

In terms of impedance cytometry, one way of increasing the sensitivity whilst maintaining a relatively large channel dimensions is to focus particles into the sensing region through the use of an insulating sheath flow; using a low conductivity liquid such as distilled water. This principle is used in Coulter counters where the sheath flow serves to concentrate the electric field lines and hence the sensing volume without restricting the physical geometry of the device. When sample focussing is achieved both vertically and laterally the size of the detection area can be precisely adjusted to suit the size of the particles being analysed, thus greatly increasing the sensitivity of the system. Hydrodynamic focussing in two dimensions allows dynamic control of aperture size, which can be varied during the experiment.[17] The first example of this type of micro-Coulter counter with variable aperture was reported by the group of Vellekoop *et al.*,[18] who used distilled water as the sheath flow fluid and increased the sensitivity by a factor of 50. However, little quantitative data were reported. Similarly micro-Coulter counters with adjustable apertures have been used to measure mixtures of beads[19,20] and to detect yeast cells.[21] Although a two-dimensionally adjustable aperture might improve the flexibility of the system, the devices presented in the literature to date suffer from a lack of accuracy, being limited by the use of coplanar electrodes. This arrangement gives a highly divergent field compared to the opposing electrode configurations.[21] The impedance signal from a particle travelling through the detection volume depends on the height of the particle in the channel, *i.e.* the distance from the electrodes.[22]

This height dependence causes an increase in the dispersion of the signal amplitude distribution, making discrimination of similarly sized particles impossible. Despite efforts to develop a sensitive and reliable micro-impedance system for analysis of particles of around 1 μm in size, to date no effective solution has been reported.

In this work we describe a micro-impedance device which has a wide channel to avoid blockage, but where the sample is sheathed with an insulating non-aqueous fluid of oil. This sheath fluid hydrodynamically focusses the sample into a region of uniform electric field, defined by the width of an inner conducting sample stream that carries particles. The concept is shown in Fig. 1, which illustrates the micro-channel where the sample flow, supplied from a central inlet, is constrained laterally by two equal streams coming from the side inlets, and forced into a narrow stream in the centre of the channel. This ensures that the suspended particles are aligned into a single file, and cross the interrogation region (two pairs of micro-electrodes located downstream) one at a time.

This method increases the sensitivity of the system without reducing the dimension of the channel. The principle of using a non-aqueous phase to confine the sample and decrease the volume of the detection volume was first suggested by Larsen *et al.*,[23] however, no measurements were presented. An issue with the technique is that the surface tension at the interface between the oil and water can cause flow instability, resulting in fluctuations of the detection volume leading to noise in the measurements. This problem was solved by adding small amount of surfactant to the organic phase, thus reducing the surface tension at the interface. We show that using this method, the sample stream can be confined to a width of ~10 μm in a 200 μm wide channel producing stable flow and noise free signals. Using a 200 μm wide channel, we demonstrate detection of 1 μm particles and discrimination between bacteria and beads of similar size.

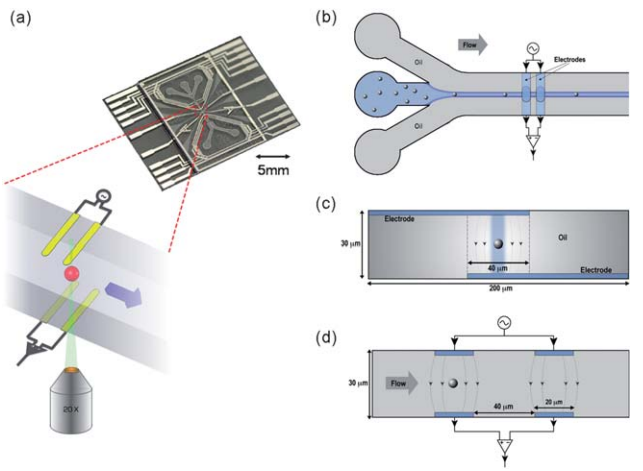


**Fig. 1** Schematic diagram showing the working principle of the micro-impedance device. (a) Two pairs of electrodes located on the top and bottom faces of the channel and overlapping in the centre of the channel are used to measure the impedance from a single particle travelling through the detection region. Fluorescence emission from the particle is recorded simultaneously. (b) Top view, (c) side view, and (d) cross-section of the micro-impedance device showing the hydrodynamic focussing system where oil is used as the sheath flow (not drawn to scale).

## Simulations

Numerical simulations were performed using COMSOL Multiphysics (ver. 3.4) to investigate the effect of focussing the sample stream (*i.e.* reducing the detection volume) and to estimate the increase in sensitivity of the system. A 2-D system was simulated with a domain consisting of a rectangle 200 μm wide and 30 μm high representing the channel cross-section. The electrodes are defined as segments of the lower and upper boundaries of the rectangle and are considered as equipotential surfaces. To investigate the effects of focussing, two situations were analysed: first with the entire volume filled with buffer solution ($\sigma = 1.6$ S m$^{-1}$, $\varepsilon_r = 78$), then with buffer occupying a central portion of the channel, equivalent to a sample stream 12 μm wide and 30 μm high. Outside this region there is oil ($\sigma = 0$ S m$^{-1}$, $\varepsilon_r = 10$). In both cases, the electric field was simulated for an applied potential of 1 V between the pair of electrodes. Plots of the current density in a cross-section of the channel are shown in Fig. 2. When the channel is filled with buffer (Fig. 2(a)), the current path is divergent and occupies most of the available channel cross-section. When the channel is filled with buffer and oil (Fig. 2(b)), the current density is confined to the high conductivity region occupied by the buffer, creating a much smaller sensing volume, and increasing the sensitivity of the system. A closer view of the current density in the channel centre is shown for each case demonstrating the field confinement.

## Experimental

Carboxylate-modified polystyrene beads were purchased from Invitrogen. They were fluorescent, orange (540/560 nm) and red (633/760 nm) with a mean diameter of 1 μm and 2 μm respectively, and a quoted coefficient of variation (CV) between 1% and

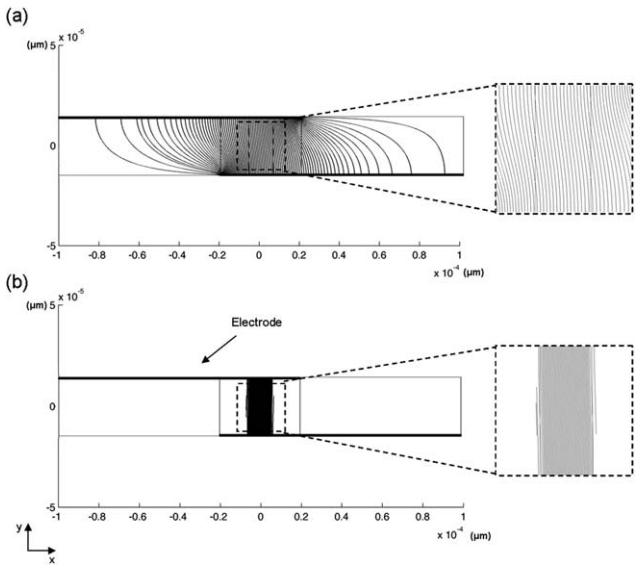


**Fig. 2** Schematic cross-section of the channel with a streamline plot of the current density obtained for a potential of 1 V applied to the top electrode and bottom electrode grounded, when the channel is filled with PBS (a), and when oil is used to confine the sample solution in the centre of the channel (b).

 

5%. The beads were washed three times in PBS and re-suspended, after sonication, in PBS (conductivity = 1.6 S $m^{-1}$). *Escherichia coli* strain BL21(DE3) expressing Ds Red protein (558/583 nm) was a gift from Dr Peter L. Roach (University of Southampton). The bacteria were inoculated into 100 ml of sterile 2YT broth (Sigma-Aldrich) containing ampicillin (Sigma-Aldrich) (100 mg $ml^{-1}$) and cultured under aerobic conditions at 37 °C with shaking (180 rpm). Growth was monitored by measuring the optical density (OD) of cell suspension at 600 nm. Expression of DS Red protein was induced by the addition of 1 mM IPTG (Isopropyl β-D-1-thiogalactopyranoside) when $OD_{600}$ reached 0.6. *E. coli* was washed and re-suspended in PBS in order to arrest cell growth and to maintain a constant concentration during the experiment. Two different samples were prepared for the measurements: (1) a mixture of 1 μm and 2 μm beads, and (2) a mixture of 2 μm beads and bacteria. For both samples, the mixture was in a ratio of 1 : 1 with a final concentration of 300 particles per μl ($3 \times 10^5$ cfu per ml).

Conventional optical flow cytometric analysis (FACS) of cells was carried out with a FACSAria (Becton Dickson) equipped with two lasers: 488 nm solid state (20 mW, Coherent® Sapphire™) and 633 nm HeNe (20 mW, JDS Uniphase™). FACSFlow sheath fluid (Becton Dickson) was used and sample flow was at a pressure of 70 psi through a 70 μm nozzle. The instrument was controlled by a PC running FACSDiVa™ software (Becton Dickson). The 1 μm and 2 μm diameter polystyrene particles were sized using Dynamic Light Scatter (DLS), using a Zetasizer Nano ZS (Malvern Instruments, UK).

The dimensions of the micro-impedance chip are shown in Fig. 1(c) and (d). The device consists of a microfluidic channel with two pairs of electrodes located on both top and bottom faces of the channel.[3,4] The chip is fabricated from glass and the electrodes are made of platinum; details of the fabrication process can be found elsewhere.[8] The channel width is 200 μm and the height 30 μm. The electrodes are 120 μm long and 20 μm wide and extend partway across the channel, overlapping in the centre (Fig. 1(c)). In the overlap region, the two electrodes define a detection volume of $40 \times 20 \times 30$ $\mu m^3$. Two pairs of electrodes are used for differential measurements (Fig. 1(b)), with a separation gap of 40 μm.

In order to improve the wettability of the channel, the channel was coated with bovine serum albumin (BSA) by flowing a 5% solution of BSA in PBS through the device for 1 hour. Flow was manually controlled using pneumatic methods similar to those described previously.[24] The applied pressure was independently controlled at each inlet; this provided flexibility and fine control of the sample stream positioning within the channel. The pressure was adjusted to give a sample stream width of 12 μm and the particle transit time through the measurement region was ~2 ms. Particles were suspended in PBS and pumped through the device using the oil/surfactant mixture (Hexandiol containing 1% Tween 20) as sheath fluid. Impedance was measured using AC signals at frequencies between 503 kHz and 5 MHz and amplitudes ranging from 3.5 $V_{pp}$ to 5 $V_{pp}$. The output from the electrodes was measured using custom built electronics and a RF lock-in amplifier (SR844, Stanford Research Instruments, USA). Fluorescence emission from the particles was detected using custom made confocal optical system,[8] with a 532 nm (20 mW solid state) and 633 nm (20 mW HeNe) laser. Two emission wavelengths were simultaneously measured: 585 ± 30 nm and 670 ± 40 nm.

The data were sampled at 120 kHz with a 16-bit A–D card (NI6034E, National Instruments) and recorded with LabVIEW™ (National Instruments, USA) software. For each experiment the number of events ranged from 3000 to 5000. The data were analysed using LabVIEW™ and post-processed in MATLAB (Mathworks Inc., Natick, USA).

## Results and discussion

Fig. 3 shows an example of the signals obtained from a 1 μm diameter polystyrene bead when an AC signal at a frequency of 503 kHz and 5 $V_{pp}$ is applied. The double peak signals correspond to the in-phase and out-of-phase components of the impedance signal. These signals are followed by a single peak that is the fluorescence signal (585 nm for the 1 μm bead) from the particle as it passes through the laser beam.

Scatter plots of the impedance (magnitude at 503 kHz) for mixtures of the beads and *E. coli* are shown in Fig. 4 and 5. Fig. 4(a) shows data for a 1 : 1 mixture of 1 μm and 2 μm beads, whilst Fig. 5(a) shows similar data for 2 μm beads and *E. coli*. The data are plotted as transit time *versus* magnitude of the impedance at 503 kHz, triggered by the in-phase impedance signal. The data are colour-coded according to the fluorescence signal (acquired simultaneously) from the particles. Both figures show that impedance can be used to discriminate between the different populations.

In conventional micro-impedance cytometry, the velocity of the particles (transit time) varies along the channel width and height, due to the parabolic flow profile of the fluid. However, Fig. 4 and 5 show that with the oil focussing, the transit times of the particles are quite similar, indicating that all the particles travel through the detection region with the same velocity. From the average of the recorded transit times, a mean particle velocity of ~38 mm $s^{-1}$ can be estimated for the 1 μm and 2 μm beads, and

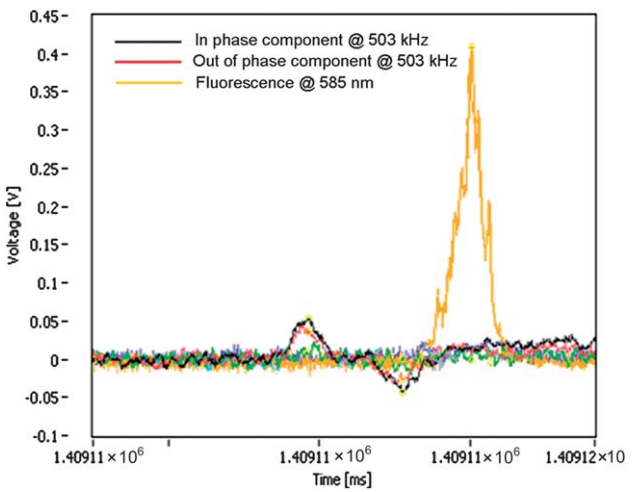


**Fig. 3** Example of impedance signals from a 1 μm diameter bead detected in the micro-flow cytometer. The real component (in phase) and imaginary component (90° out of phase) of the electrical impedance at the applied frequency are shown. Orange (585/40 nm) fluorescence emission is also shown.

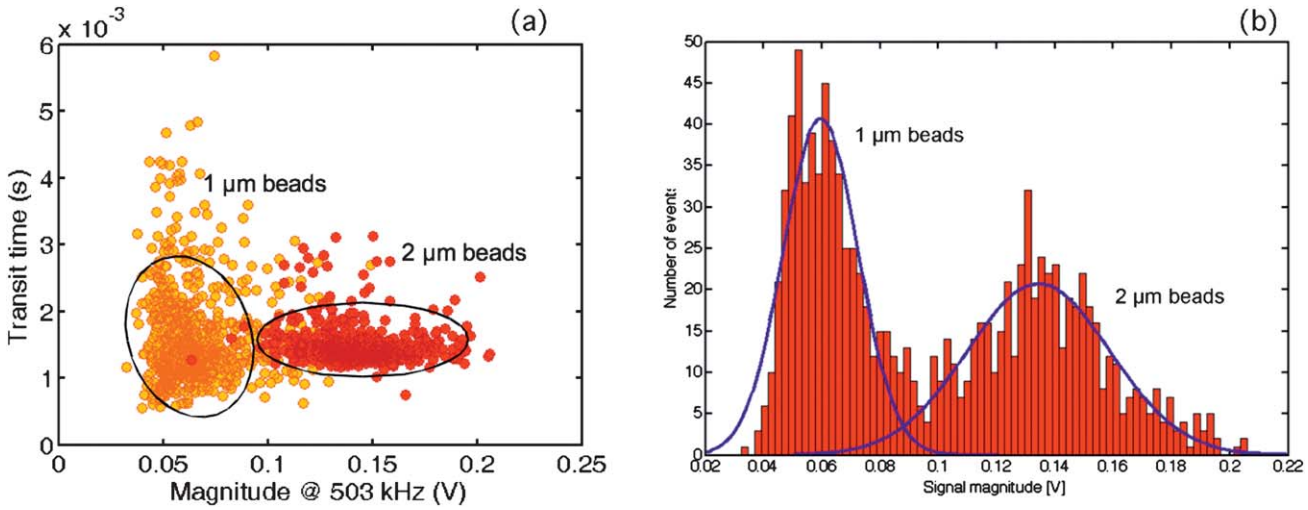


**Fig. 4** (a) Scatter plot of particle transit time against magnitude of the impedance at 503 kHz for a mixture of 1 μm and 2 μm diameter polystyrene beads. The plot is colour coded based on the fluorescence measured from each bead. (b) Histograms of the impedance amplitudes for the mixtures of 1 μm and 2 μm diameter polystyrene beads measured at 503 kHz.

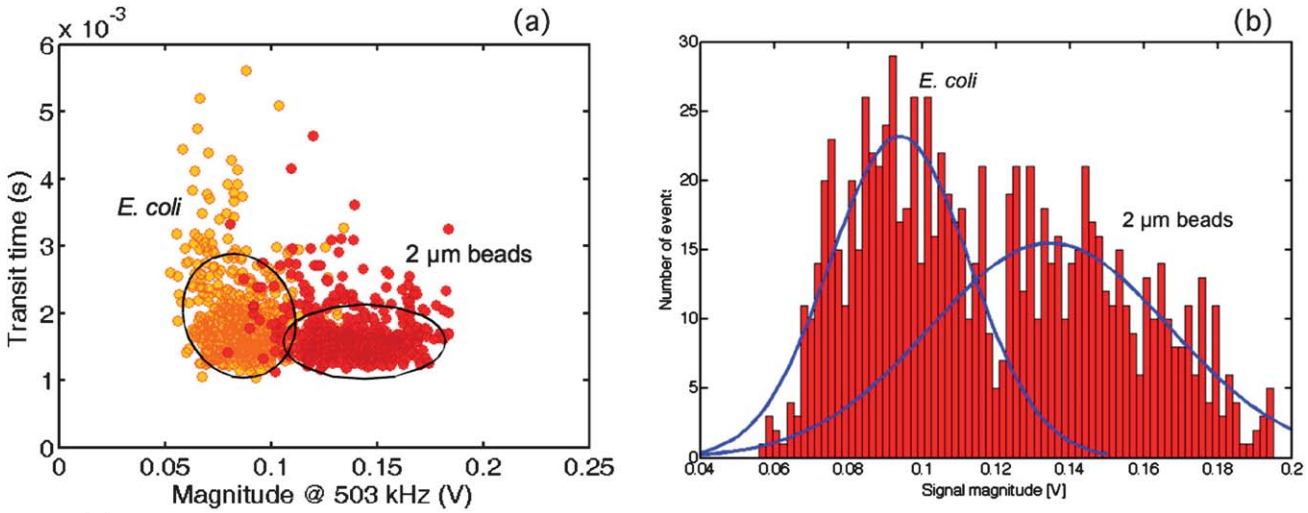


**Fig. 5** (a) Scatter plot of particle transit time against magnitude of the impedance at 503 kHz for a mixture of *E. coli* and 2 μm diameter polystyrene beads. The plot is colour coded based on the fluorescence measured from each particle. (b) Histograms of the impedance amplitudes for the mixtures of *E. coli* and 2 μm diameter polystyrene beads measured at 503 kHz.

~32 mm $s^{-1}$ for 2 μm beads and *E. coli* mix; equivalent to a flow rate of approximately 0.8 μl $min^{-1}$ and 0.7 μl $min^{-1}$, respectively. The volume of sample analysed during an experiment is obtained by multiplying the flow rate by the time of measurement (19 min for the mixture of beads, and 17 min for the mixture of beads and *E. coli*). Dividing the number of events by sample volume shows that for both samples, the concentration of particles was approximately 10% lower than calculated from the stock solutions. This small discrepancy could be due to an error in the calculation of the cross-sectional area of the channel (and the volumetric flow rate) due to the unknown shape of the meniscus formed at the oil/buffer interface (assumed to be a square cross-section in the calculations).

Fig. 4(b) and 5(b) show histograms of the number of events plotted against the magnitude of the impedance (503 kHz). These impedance histograms were fitted to a linear combination of two Gaussian distributions using the standard algorithms found in the MATLAB curve fitting tools. For the bead mixture (Fig. 4), two clearly separated distributions are obtained. For *E. coli* and 2 μm beads, the fits produce less well defined populations. The 2 μm bead distribution overlaps into the *E. coli* population, this is probably due to the wide spread in the size of the *E. coli*. The organism is typically 2 μm long by 0.5 μm wide so that orientation effects may also influence the impedance signal. These Gaussian fits were performed on the complete impedance dataset without bias. However, Fig. 5(a) shows that the *E. coli* population is clearly delineated from the bead population when the fluorescence signal is considered.

From these fits, the number of particles in each distribution was estimated. The same analysis was also performed with



 

**Table 1** Summary data for mixture of beads (Fig. 4) and beads and *E. coli* (Fig. 5). Table shows mean amplitude ($\mu$), coefficient of variation (CV), and % determined from the fitted Gaussian distributions for data triggered on impedance or fluorescence signals. For comparison, the % population and CV obtained from fluorescence flow cytometry (FACS) are shown, together with the size CV obtained from Dynamic Light Scatter (DLS) and the manufacturers CV

| | Impedance (micro-flow cytometer) | | | | Fluorescence (micro-flow cytometer) | | | Fluorescence (FACS) | | DLS | Data from manufacturer |
|---|---|---|---|---|---|---|---|---|---|---|---|
| | $\mu$/V | CV | Calculated CV in size | No. % | $\mu$/V | CV | No. % | CV | No. % | CV | CV |
| 1 μm beads | 0.060 | 22% | 8% | 54.3 | 0.060 | 22% | 57.8 | 28.8% | 60.0 | 8% | 5% |
| 2 μm beads | 0.134 | 19% | 6% | 45.7 | 0.140 | 14% | 42.2 | 17.1% | 40.0 | 8% | 5% |

| | Impedance (micro-flow cytometer) | | | | Fluorescence (micro-flow cytometer) | | | Fluorescence (FACS) | | DLS | Data from manufacturer |
|---|---|---|---|---|---|---|---|---|---|---|---|
| | $\mu$/V | CV | Calculated CV in size | No. % | $\mu$/V | CV | No. % | CV | No. % | CV | CV |
| *E. coli* | 0.094 | 20% | 6% | 55.2 | 0.091 | 19% | 52.4 | 50.1% | 53.0 | — | — |
| 2 μm beads | 0.135 | 23% | 7.5% | 44.8 | 0.147 | 16% | 47.6 | 21.2% | 47.0 | 8% | 5% |



particles identified from their fluorescence signal rather than impedance. These data together with the CVs are summarised in Table 1. The particle size distribution and fluorescence intensity distribution were also measured by Dynamic Light Scattering (DLS) and conventional flow cytometry (FACS), respectively. FACS sizes particles based on the forward scattered light intensity, but the 1 μm and 2 μm beads were too small to reliably measure using this technique; DLS was therefore used to measure particle size. Examination of the CV of fluorescence intensity (measured by FACS and micro-cytometer) shows that the particles have a wide distribution in fluorescence, but the CV from both the FACS and the micro-cytometer are similar. The CV of the size measurements obtained from DLS is slightly higher than the manufacturer quoted values, but lower than the 503 kHz impedance CV. This apparent discrepancy is explained as follows.

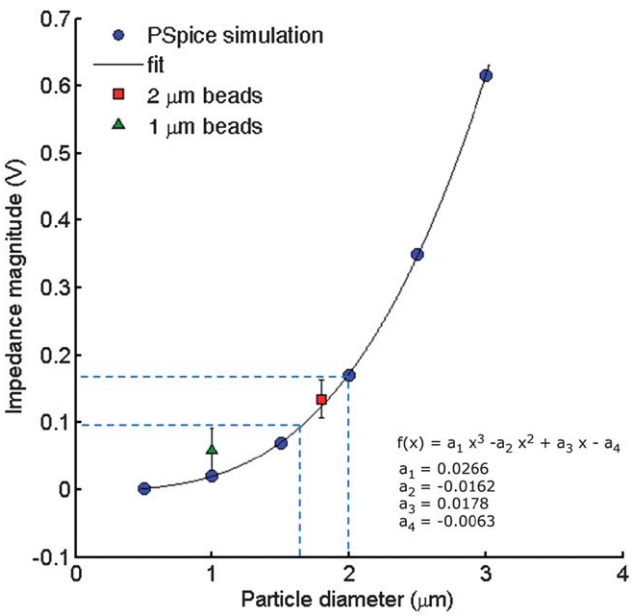


**Fig. 6** Plot showing the correlation between the particle size and the magnitude of the impedance signal. The data points were obtained from PSpice circuit simulations for different sizes of beads, including the equivalent circuit model for a bead suspended in the detection region and the amplification electronics. The curve is a third order polynomial fit. Bead permittivity = $2.55\varepsilon_o$ and surface conductivity = 1.2 nS. The permittivity and conductivity of the suspending medium were 80 and 1.6 S m$^{-1}$, respectively.

To a first approximation, the magnitude of the low frequency impedance can be considered proportional to particle volume.[5,6,25] A calculation showing the relationship between particle size and impedance magnitude is plotted in Fig. 6. The data points were obtained from PSpice circuit simulations for different sizes of beads, based on the full equivalent circuit model for a bead suspended in the detection region and including the electrical properties of the amplification electronics.[6,9,25] The curve is a third order polynomial fit and shows that as the particle size decreases, there is an approximately cubic decrease in impedance magnitude, tending towards zero for the smaller particles. The measured impedance value for the 1 μm and 2 μm beads is also plotted on the figure. From DLS data, the 2 μm particle has an actual diameter of 1.8 μm, and this impedance point fits on the calculated curve. The measured impedance for the 1 μm particle is higher than calculated. This could be due a number of sources of error, for example an accurate estimate of the volume fraction depends on the knowledge of the exact shape of the oil–water boundary. Also as the particle size gets smaller, numerical errors become more significant.

The curve was fitted to a third order polynomial, and from this the CV in size was estimated from the measured impedance data. These data are listed in Table 1, as "Calculated CV in size". These size CVs are very close to the data obtained from DLS, and also the manufacturer's data for the polystyrene particles. The CV in size for the *E. coli* was also estimated from Fig. 6, and shows that the bacteria have a tight distribution, which is to be expected as they are in stationary phase.

## Conclusions

We have demonstrated a microfluidic impedance cytometer that uses an insulating fluid of oil to hydrodynamically focus particles into the centre of a 200 μm wide channel. This technique was shown to significantly increase the sensitivity of the system whilst

maintaining large channel dimensions which do not block. Assuming that the PBS sample is sheathed with oil with vertical walls, the volume ratio of particle to sensing volume is estimated to be 0.007%. Measurement of the impedance from single particles is used to discriminate between 1 μm and 2 μm diameter beads and *E. coli* and 2 μm beads. Accurate detection and identification of the particles were confirmed by simultaneously measuring the fluorescence emission. The distribution in size and fluorescence (CV) is found to be in good agreement with data obtained from standard commercially available instruments (FACS and DLS).

## Acknowledgements

We thank Dr P. L. Roach and Dr R. Wood for providing *E. coli* cells. We are grateful to Dr T. Newman for helpful discussions. We thank Andrew Whitton for fabrication of the microfluidic chip and Philips for software development.

## Notes and references

1 H. E. Ayliffe, A. B. Frazier and R. D. Rabbitt, *J. Microelectromech. Syst.*, 1999, **8**, 50–57.
2 S. Gawad, L. Schild and P. Renaud, *Lab Chip*, 2001, **1**, 76–82.
3 H. Morgan, D. Holmes and N. G. Green, *Curr. Appl. Phys.*, 2006, **6**, 367–370.
4 T. Sun, D. Holmes, S. Gawad, N. G. Green and H. Morgan, *Lab Chip*, 2007, **7**, 1034–1040.
5 K. Cheung, S. Gawad and P. Renaud, *Cytometry, Part A*, 2005, **65**, 124–132.
6 T. Sun, C. Bernabini and H. Morgan, *Langmuir*, 2010, **26**(6), 3821–3828.
7 H. Morgan, T. Sun, D. Holmes, S. Gawad and N. G. Green, *J. Phys. D: Appl. Phys.*, 2007, **40**, 61–70.
8 D. Holmes, J. K. She, P. L. Roach and H. Morgan, *Lab Chip*, 2007, **7**, 1048–1056.
9 D. Holmes, D. Pettigrew, C. H. Reccius, J. D. Gwyer, C. van Berkel, J. Holloway, D. E. Davies and H. Morgan, *Lab Chip*, 2009, **9**, 2881–2889.
10 N. Watkins, B. M. Venkatesan, M. Toner, W. Rodriguez and R. Bashir, *Lab Chip*, 2009, **9**, 3177–3184.
11 X. Wu, Y. Kang, Y. N. Wang, D. Xu, D. Y. Li and D. Q. Li, *Electrophoresis*, 2008, **29**, 2754–2759.
12 R. W. Deblois and C. P. Bean, *Rev. Sci. Instrum.*, 1970, **41**, 909–916.
13 R. W. Deblois, C. P. Bean and R. K. A. Wesley, *J. Colloid Interface Sci.*, 1977, **61**, 323–335.
14 R. W. Deblois and R. K. A. Wesley, *J. Virol.*, 1977, **23**, 227–233.
15 O. A. Saleh and L. L. Sohn, *Proc. Natl. Acad. Sci. U. S. A.*, 2003, **100**, 820–824.
16 O. A. Saleh and L. L. Sohn, *Nano Lett.*, 2003, **3**, 37–38.
17 G. Hairer and M. J. Vellekoop, *Microfluid. Nanofluid.*, 2009, **7**, 647–658.
18 J. H. Nieuwenhuis, F. Kohl, J. Bastemeijer, P. M. Sarro and M. J. Vellekoop, *Sens. Actuators, B*, 2004, **102**, 44–50.
19 J. H. Nieuwenhuis, P. Svasek, P. M. Sarro and M. J. Vellekoop, *Technical Digests of Eurosensors*, 2004, **XVIII**, 317–320.
20 R. Scott, P. Sethu and C. K. Harnett, *Rev. Sci. Instrum.*, 2008, **79**, 046104.
21 R. Rodriguez-Trujillo, O. Castillo-Fernandez, M. Garrido, M. Arundell, A. Valencia and G. Gomila, *Biosens. Bioelectron.*, 2008, **24**, 290–296.
22 T. Sun, N. G. Green, S. Gawad and H. Morgan, *IET Nanobiotechnol.*, 2007, **1**, 69–79.
23 U. D. Larsen, G. Blankenstein and J. Branebjerg, *Proc of Transducers '97*, Chicago, USA, June 16–19, 1997, pp. 1319–1322.
24 T. Braschler, L. Metref, R. Zvitov-Marabi, H. van Lintel, N. Demierre, J. Theytaz and P. Renaud, *Lab Chip*, 2007, **7**, 420–422.
25 T. Sun, G. Gawad, N. G. Green and H. Morgan, *J. Phys. D: Appl. Phys.*, 2007, **40**, 1–8.



 